Rate Constant for the Recombination Reaction $CH_3 + CH_3 \rightarrow C_2H_6$ at $T = 298$ and 202 K

Regina J. Cody,*,† Walter A. Payne, Jr.,† R. Peyton Thorn, Jr.,‡ Fred L. Nesbitt,§ Mark A. Iannone,|| Dwight C. Tardy,⊥ and Louis J. Stief†

Laboratory for Extraterrestrial Physics, NASA/Goddard Space Flight Center, Greenbelt, Maryland 20771, Department of Natural Sciences, Coppin State College, Baltimore, Maryland 21216, Department of Chemistry, Millersville University, Millersville, Pennsylvania 17551, and Department of Chemistry, University of Iowa, Iowa City, Iowa 52242

Received: November 2, 2001; In Final Form: March 19, 2002

The recombination of methyl radicals is the major loss process for methyl in the atmospheres of Saturn and Neptune. The serious disagreement between observed and calculated levels of CH_3 has led to suggestions that the atmospheric models greatly underestimated the loss of CH_3 due to poor knowledge of the rate of the reaction $CH_3 + CH_3 + M \rightarrow C_2H_6 + M$ at the low temperatures and pressures of these atmospheric systems. In an attempt to resolve this problem, the absolute rate constant for the self-reaction of CH_3 has been measured using the discharge-flow kinetic technique coupled to mass spectrometric detection at $T = 202$ and 298 K and $P = 0.6-2.0$ Torr nominal pressure (He). CH_3 was produced by the reaction of F with CH_4, with $[CH_4]$ in large excess over [F], and detected by low energy (11 eV) electron impact ionization at $m/z = 15$. The results were obtained by graphical analysis of plots of the reciprocal of the CH_3 signal vs reaction time. At $T = 298$ K, $k_1(0.6\ \text{Torr}) = (2.15 \pm 0.42) \times 10^{-11}$ cm^3 molecule^{-1} s^{-1} and $k_1(1\ \text{Torr}) = (2.44 \pm 0.52) \times 10^{-11}$ cm^3 molecule^{-1} s^{-1}. At $T = 202$ K, the rate constant increased from $k_1(0.6\ \text{Torr}) = (5.04 \pm 1.15) \times 10^{-11}$ cm^3 molecule^{-1} s^{-1} to $k_1(1.0\ \text{Torr}) = (5.25 \pm 1.43) \times 10^{-11}$ cm^3 molecule^{-1} s^{-1} to $k_1(2.0\ \text{Torr}) = (6.52 \pm 1.54) \times 10^{-11}$ cm^3 molecule^{-1} s^{-1}, indicating that the reaction is in the falloff region. Klippenstein and Harding had previously calculated rate constant falloff curves for this self-reaction in Ar buffer gas. Transforming these results for a He buffer gas suggest little change in the energy removal per collision, $-\langle\Delta E\rangle_d$, with decreasing temperature and also indicate that $-\langle\Delta E\rangle_d$ for He buffer gas is approximately half of that for Argon. Since the experimental results seem to at least partially affirm the validity of the Klippenstein and Harding calculations, we suggest that, in atmospheric models of the outer planets, use of the theoretical results for k_1 is preferable to extrapolation of laboratory data to pressures and temperatures well beyond the range of the experiments.

Introduction

The methyl radical recombination reaction is one of the most studied in the field of chemical kinetics. The experimental and theoretical studies are far too numerous to list individually. The NIST 1998 Kinetics Data Base[1] lists more than 60 references for this reaction. Noteworthy is the classic 1951 paper by Gomer and Kistiakowsky[2] using the rotating sector technique in a photodecomposition experiment that may be considered the first reliable quantitative measurement of the high-pressure rate constant k_∞.

For present purposes we mention three extensive experimental studies which are frequently cited. Macpherson, Pilling, and Smith[3] (1983, 1985) measured the rate constant at $T = 296-577$ K and $P = 5.4-500$ Torr Ar in laser photolysis−UV absorption (LP−UVA) experiments; Table IV of the 1985 paper gives a good summary of experimental results for the period 1969−1980. They determined k_∞ (296 K) $= 6.5 \times 10^{-11}$ cm^3 molecule^{-1} s^{-1} with a small negative temperature dependence given by $k_\infty = 4.1 \times 10^{-11} \exp(137/T)$; values for k_0 were also reported. To obtain more detailed knowledge of this reaction in the falloff region, Slagle et al.[4] (1988) employed two techniques. In laser photolysis−photoionization mass spectrometry (LP−PIMS) studies, the rate constant was measured at $T = 296-906$ K, $P = 1.2-10.6$ Torr Ar and at $T = 296-810$ K, $P = 2.5-10.7$ Torr He. In LP−UVA studies, the experimental conditions were $T = 296-906$ K and $P = 5.4-493$ Torr Ar. Analytical expressions for k_0 as a function of temperature and pressure (M = Ar) and k_∞ as a function of temperature were presented. Both sets of measurements suggest k_∞ (296 K) $= 6.0 \times 10^{-11}$ cm^3 molecule^{-1} s^{-1}. Walter et al.[5] (1990) reported measurements at $T = 200$, 300, and 408 K in Ar buffer gas. In LP−UVA experiments at $T = 200$ K and $P = 9.6-401$ Torr, the high-pressure limiting rate constant k_∞ (200 K) $= 6.9 \times 10^{-11}$ cm^3 molecule^{-1} s^{-1}. In discharge flow−mass spectrometry (DF−MS) experiments they reported pressure dependent k values in the range $(1.7-4.1) \times 10^{-11}$ cm^3 molecule^{-1} s^{-1} at $T = 300$ K, $P = 0.15-2.2$ Torr Ar and in the range $(1.1-2.9) \times 10^{-11}$ cm^3 molecule^{-1} s^{-1} at $T = 408$ K, $P = 0.3-3.2$ Torr Ar.

Among the many theoretical studies of the methyl recombination reaction are those by Wardlaw and Marcus[6] (1986), Wagner and Wardlaw[7] (1988), Forst[8] (1991), Robertson et al.[9]

* Corresponding author. Mailing address: NASA/Goddard Space Flight Center, Code 691, Greenbelt, MD 20771. Tel: 301-286-3782. Fax: 301-286-0212. E-mail: regina.cody@gsfc.nasa.gov

† Goddard Space Flight Center.

‡ Present address: The Midland Certified Reagent Company, 3112-A W. Cuthbert Ave., Midland, TX 79701.

§ Coppin State College.

|| Millersville University.

⊥ University of Iowa.

10.1021/jp014044l CCC: $22.00
Published on Web 06/01/2002

(1995), and Klippenstein and Harding[10] (1999). The RRKM calculations of Wardlaw and Marcus[6] are able to account for the experimentally observed negative temperature dependence of k_∞ at $T = 300-2000$ K. At $T = 300$ K, $k_\infty = 7.1 \times 10^{-11}$ cm^3 $molecule^{-1}$ s^{-1}. The Wagner and Wardlaw[7] variational RRKM theory calculations were performed in conjunction with the experimental study by Slagle et al.[4] In the Wagner and Wardlaw[7] calculations as well as the microcanonical variational theory calculations of Forst,[8] good agreement is observed between the Slagle et al.[4] experiments and the calculations in the range $T = 296-906$ K and $P = 5.4-493$ Torr Ar. The calculations by Robertson et al.[9] include results for k_∞ at $T = 200$ K but not for k_0. Extensive master equation calculations using an ab initio potential energy surface and the RRKM model by Klippenstein and Harding[10] provide values for k over a wide pressure range ($P = 0.1-1000$ Torr Ar) and at $T = 200-1700$ K. Although they find that k_∞ decreases with increasing temperature for $T > 296$ K, the value for k_∞ between $T = 296$ and 200 K is essentially constant at 6.4×10^{-11} cm^3 $molecule^{-1}$ s^{-1}.

The impetus for the present study was the recent detection of the methyl free radical in the atmospheres of Saturn[11] and Neptune.[12] These are the first observations of any free radical in the atmospheres of the outer planets. The levels of CH_3 observed were much lower than predicted by atmospheric models, especially for Saturn. It has been suggested[11-14] that the models greatly underestimated the loss of CH_3 due to poor knowledge of the rate of the self-reaction

$$CH_3 + CH_3 + M \rightarrow C_2H_6 + M \qquad (1)$$

at the low temperatures and pressures of these atmospheric systems. For the atmospheric models, appropriate conditions would be $T = 140-200$ K, $P < 0.2$ Torr, and M = H_2/He.

Laboratory data used in the models came essentially from the studies of Slagle et al.[4] With few exceptions, most laboratory studies have been performed at higher temperatures ($T \geq 296$ K) or higher pressures ($P \geq 5$ Torr) or with inappropriate bath gases M (usually Ar). Only two reports are available of studies below room temperature and both are at the high-pressure limit (k_∞): the results of Walter et al.[5] at $T = 200$ K, $P = 9.6-401$ Torr Ar and those of Parkes et al.[15] at $T = 253$ and 273 K, $P = 760$ Torr N_2. We are aware of only a few published studies at pressures below 5 Torr. They include the extensive DF−MS results of Walter et al.[5] at $P = 1.1-4.1$ Torr Ar and the LP−PIMS results of Slagle et al.[4] at $P = 1.2-10.6$ Torr Ar and $P = 2.5-10.7$ Torr He. There are also studies in which results for reaction 1 were a byproduct of the main study of the reaction of CH_3 with a free radical R with $[CH_3] > [R]$. These include the discharge flow−laser magnetic resonance (DF−LMR) results of Deters et al.[16a,b] at $P = 0.5-3.0$ Torr He and the recent LP−PIMS results of Stoliarov et al.[16c] at $P = 0.94-3.8$ Torr He. Finally, the only published studies employing He as a bath gas are those of Slagle et al.,[4] Deters et al.,[16a,b] and Stoliarov et al.[16c] The paucity of data at low temperatures and low pressures reflects both experimental convenience and the importance of the $CH_3 + CH_3$ reaction in hydrocarbon combustion chemistry.

We report here on measurements of k_1 using the DF−MS technique. Experiments at $T = 298$ K and $P = 0.6$ and 1.0 Torr He may be compared with the few previous low-pressure studies with M = He. We have also measured k_1 at $T = 202$ K and $P = 0.6-2.0$ Torr He (the limits of our system), which provides the first measurements of this rate constant in the falloff region at $T < 296$ K. This allows for verification of the recent calculations by Klippenstein and Harding[10] on the pressure dependence of k_1 at $T = 200$ K when modified from M = Ar to M = He.

Experimental Section

Discharge Flow Reactor. The experiments were performed in a Pyrex flow tube about 60 cm in length and 2.8 cm in diameter. The inner surface of the flow tube was lined with Teflon FEP. The flow tube was fitted with a Pyrex movable injector whose position could be varied between a distance $d = 2$ and 44 cm from the sampling pinhole. The system has been described in previous publications.[17,18]

The flow tube was used at ambient temperature or cooled by circulating ethanol from a cooled reservoir through the jacket surrounding the tube. At $T = 202$ K the temperature profile is flat ($\pm$ 2 K) from $d = 10$ to 44 cm. However, there is a gradual increase in temperature in the region $d = 1-10$ cm where the flow tube is coupled to the MS sampling system. Modeling calculations show that the higher temperatures in this region have little or no effect on the reaction chemistry since we are studying a rather fast reaction. However, the flow velocity varies directly with T, and thus the time scale is distorted in this region close to the sampling pinhole. This time perturbation has been shown to have little effect on the exponential decay of signal under the usual pseudo-first-order conditions. But in the present experiments with signal decay under mostly second-order conditions, the distortion of the decay profile was evident and the decay was difficult to fit with either a pure second-order plot of $1/[CH_3]$ vs time or the numerical simulation program described in the results section. Corrected reaction times were obtained by numerically integrating the inverse of the position-dependent flow velocity from the pinhole to each injector position. When analyzed in this way, all the $T = 202$ K experiments gave signal profiles free of distortion.

In addition to the effect on reaction chemistry and flow velocity, the effect of the temperature gradient on the number density or concentration of CH_3 is a potential problem. Extensive calculations using a simple model were performed in which the temperature from $d = 10$ cm to the mass spectrometer sampling pinhole at $d = 0$ cm was increased linearly at 2 cm intervals as observed in our system. For the conditions of our experiments, the calculations showed that for $d \geq 10$ cm, the slope of the $1/[CH_3]$ vs time plot was the same as that for the case of no temperature gradient but the line was slightly displaced downward. For $d = 10$ cm, the line showed slight upward curvature. For several reasons, this effect was rendered negligible under the conditions and practices of our experiments. First, the deviation at $d = 8$ or 9 cm from the straight line is small and well within the scatter of the data. In addition, we did not attempt to record data for $d = 2$ cm due to end effects and flow perturbations in the pump out region near the sampling pinhole. For the remaining two or three points in the interval $d = 3$ to 7 cm, we frequently observed upward curvature in the $1/[CH_3]$ vs time plot and neglected these data points. The observed upward curvature looked very much like that predicted in the temperature gradient region. The significant conclusion is that, under the conditions of our experiments and with the routine neglect of two or three data points in the interval $d = 3$ to 7 cm, there is no measurable effect of the change in $[CH_3]$ on the slope of the $1/[CH_3]$ vs time plots, and hence no measurable effect on the derived value of k_1.

The flow tube was coupled via a two-stage stainless steel collision-free sampling system to a quadrupole mass spectrometer (ABB Extrel). The CH_3 reactant, whose production is

discussed below, was monitored at low electron energies (11 eV) in order to avoid formation of CH_3^+ from dissociative ionization of CH_4 that was present in great excess. The low electron energy of 11 eV also precludes formation of CH_3^+ from dissociative ionization of the equilibrated C_2H_6 product. Ions were detected by an off-axis channeltron multiplier (Burle Electro-Optics).

Helium carrier gas was flowed into the reaction flow tube through ports at the rear end of the flow tube. All gas flows were measured and controlled by mass flow controllers (MKS Instruments). The linear flow velocity ranged from about 2400 to 2700 cm s^{-1} for the kinetic experiments at nominal pressures of 1.0 and 2.0 Torr and about 2100 cm s^{-1} for a pressure of 0.6 Torr. In the calculation of the linear flow velocity, the plug flow assumption was made. The flow velocity is calculated from the gas constant, temperature, cross-sectional area of the flow tube, total gas flow, and total pressure. A sidearm, at the upstream end of the flow tube, contained a microwave discharge for the production of F atoms. The discharge region consisted of a 3/8 in. i.d. ceramic tube coupled via Teflon Swagelok connectors to a glass discharge arm.

Production and Monitoring of CH_3. Fluorine atoms were produced at the upstream end of the flow reactor by passing molecular F_2 diluted in He through a microwave discharge (50 W, 2450 MHz). For $[F_2] \geq 1 \times 10^{12}$ molecule cm^{-3}, about 50−90% of the F_2 was dissociated in the discharge. The CH_4 reactant was admitted via a Pyrex movable injector. At the tip of the movable injector CH_3 was produced via the reaction

$$F + CH_4 \rightarrow CH_3 + HF \qquad (2)$$

where k_2 (298 K) $= 6.7 \times 10^{-11}$ and k_2 (202 K) $= 4.4 \times 10^{-11}$, both in units cm^3 $molecule^{-1}$ s^{-1} (ref 19). Methane was in large excess with concentrations in the range $(0.5-1.0) \times 10^{15}$ molecule cm^{-3}. These conditions ensured rapid and quantitative conversion of F to CH_3. Thus the large excess of CH_4 prevented secondary loss of CH_3 via reaction with F. In addition, the subsequent reaction of CH_3 with residual F_2 to form $CH_3F + F$ is followed by very rapid regeneration of CH_3 via reaction 2. The large concentrations of CH_4 required to achieve these desirable features were only possible in the present experiments due to the complete absence of dissociative ionization of CH_4 to yield CH_3^+.

Methyl radicals were detected at $m/z = 15$ following low-energy electron ionization. Mass scans were recorded for the region 14.5−15.5 amu and signals were taken as the integrated area of the $m/z = 15$ peak. Signals were typically averaged for 30−60 s for each injector position and several scans were recorded for each position. The observed signal was corrected for a small (≤1%) background signal measured with the microwave discharge off. The background signal and the background pressure in the ionization region were reduced by the use of a cold shroud (77 K) that surrounded the mass spectrometer.

Determination of $[F]_0$. The absolute concentration of fluorine atoms used to generate CH_3 was determined by measuring the consumption of Cl_2 in the fast titration reaction:

$$F + Cl_2 \rightarrow Cl + FCl \qquad (3)$$

where $k_3 = 6.2 \times 10^{-11}$ cm^3 $molecule^{-1}$ s^{-1} at $T = 298$ and 202 K.[20] The $F + Cl_2$ reaction system is ideal for this purpose. There is complete absence of complicating secondary chemistry such as Cl + residual F_2 or F + FCl since these reactions are negligibly slow. The initial F atom concentration was determined by measuring the decrease in the Cl_2^+ signal ($m/z = 70$, electron energy = 14 eV) when the microwave discharge was initiated. The dilute Cl_2/He mixture was admitted to the flow tube via the movable injector. The position of the injector was chosen to ensure that reaction 3 went to completion and that the position was close to the middle of the decay range for the CH_3 reactant. Separate experiments showed that the absolute value of $[F]_0$ was invariant for injector positions of 10 to 40 cm from the sampling pinhole. The absolute F concentration is given by

$$[F]_0 = [Cl_2]_{\text{disch. off}} - [Cl_2]_{\text{disch. on}}$$
$$\equiv \Delta[Cl_2] \text{ signal} \times [Cl_2]_{\text{disch. off}}$$

where $\Delta[Cl_2]$ signal is the fractional decrease in the Cl_2^+ signal, $(S_{\text{disch. off}} - S_{\text{disch. on}})/S_{\text{disch. off}}$. The uncertainty in $[F]_0$ is estimated to be ±10%. At low $[F]_0$ levels, the procedure was modified as described in the next section.

MS Scaling Factor for CH_3. The scaling factor for CH_3 is the ratio of the absolute $[CH_3]$ to the mass spectrometer signal at $m/z = 15$. However, the absolute $[CH_3]$ comes from the F atom titration and hence gives $[CH_3]$ at $t = 0$ while the signal is recorded at $t =$ about 3 ms and beyond due to the limitation of finite time for mixing at the tip of the injector and perturbations in the flow near the end of the flow tube. For the case of a first-order signal decay, this is readily handled by a short, linear extrapolation of the signal back to $t = 0$ in a plot of ln(signal) vs t. This is not an option in the present experiments since the signal decay is mostly second order ($CH_3 + CH_3$) but with some first-order components ($CH_3 + F_2$, CH_3 + wall; see results section). After trying several less satisfactory options to obtain $[CH_3]$ and CH_3 signal at the same time (not necessarily $t = 0$), we adopted the following procedure. We reduced $[CH_3]$ to the lowest signal level where it was still possible to quantitatively record signal decay. For the present conditions this was $[CH_3] = (2-4) \times 10^{11}$ molecule cm^{-3}. Under these conditions, the signal appears to exhibit good first-order decay although modeling shows that there is a substantial second-order contribution. To verify the correctness of this procedure, we also performed more than half of these experiments with $[Cl_2] = (2-3) \times 10^{13}$ molecule cm^{-3}, i.e., $[Cl_2] \gg [CH_3]$. Under these conditions, CH_3 decays largely by the reaction

$$CH_3 + Cl_2 \rightarrow CH_3Cl + Cl \qquad (4)$$

(See ref 21.) Thus the signal decay is strictly first-order and we determine the CH_3 signal at $t = 0$ directly by a short linear extrapolation. A small correction (5%) was made to allow for the occurrence of $F + Cl_2$ in competition with $F + CH_4$. For experiments at $T = 202$ K, we also applied a correction for the effect of increasing flow velocity due to increasing temperature in the region near the sampling pinhole as described above for the second-order decay of CH_3. As expected, the slope is not affected but the intercept is. Regeneration of CH_3 via the slow reaction of Cl with CH_4 was entirely negligible. We found that the CH_3 signal level at $t = 0$ was the same within ±10% in both the presence and absence of Cl_2. At these lower signal levels, the CH_3 background signal was more significant but could be reduced to ~10% of the observed signal as needed by pretreating the system under conditions similar to those employed for the decay of CH_3 in the presence of excess Cl_2.

The potential effect of the change in $[CH_3]$ due to the temperature gradient near the sampling pinhole, discussed in a previous section for the measurement of k_1 from the second-order decay of CH_3, must also be considered for the determi-

nation of the MS scaling factor via the first-order decay of low levels of CH_3 in the presence of excess Cl_2. Also, since the reaction $CH_3 + Cl_2$ (4) is slower than $CH_3 + CH_3$ (2) and has a stronger temperature dependence,[21] allowance must be made for the effect of the varying temperature near the pinhole on k_4. As described above, the measurement of interest here is the intercept of the ln(CH_3 signal) vs time plot, which provides the CH_3 signal at $t = 0$. Since the decay under these conditions was quite slow, we usually recorded only one or two data points in the temperature gradient region ($d = 1-10$ cm) and these were frequently neglected because they fell measurably below the trend of the other points ($d = 10-44$ cm). We saw no evidence for deviation from linearity in these plots for the constant temperature region. Extensive calculations, similar to those described for the k_1 determination, were performed using a simple model. For the conditions of our experiments, calculations showed that the CH_3 signal at $t = 0$ was lowered by only 2−3% due to the effect of changing [CH_3] and k_4 with temperature. As expected for a pseudo-first-order reaction, the slope is unchanged. The difference between the intercept with and without a temperature gradient is just the difference in the amount of reaction that occurs over the 10 cm length with and without the temperature gradient. This difference is small since there are two compensating terms in the reaction rate with the temperature gradient: increasing the temperature decreases [CH_3] and increases k_4. Thus the compensation gives a rate which is close to the amount of reaction that would have taken place if there was not a temperature gradient.

To relate the signal at $t = 0$ to $[CH_3]_0$ we need to determine $[F]_0$ at this lower level via the procedure outlined above for higher levels of $[F]_0$. However, determination of the consumption of Cl_2 in the fast titration reaction $F + Cl_2$ is not straightforward at low levels of [F]. If there is sufficient Cl_2 to ensure complete removal of F by the middle of the CH_3 decay range ($d = 20$ cm), then the consumption of Cl_2 will be immeasurably small (<1%). By moving the injector out to $d =$ 44 cm, we were able in many instances to achieve essentially complete removal of F. In some instances in which [Cl_2] was rather low, a 10−15% correction for undertitration was made. Separate experiments showed that, when corrected for undertitration of F by Cl_2, the derived [F] was constant to ±5% between $d = 20$ and 44 cm.

By combining the signal level at $t = 0$ with the value for $[F]_0$ as determined by F atom titration at the low level of $(2-4) \times 10^{11}$ molecule cm^{-3}, we obtain the desired scaling factor SF = $[CH_3]_0$/CH_3 signal. This scaling factor is then used in the graphical analysis of the $CH_3 + CH_3$ decay experiments at high [CH_3] as described below in the Results section. This of course makes the assumption that the scaling factor is the same at both high $[CH_3] = (1-10) \times 10^{12}$ molecule cm^{-3} and low $[CH_3] = (2-4) \times 10^{11}$ molecule cm^{-3}. This requires a linear dependence of signal on concentration, which is inherent in the extraction of a rate constant from the signal decay in this as well as most kinetic experiments and has been well established for mass spectrometric detection.

Materials. Helium (99.9995%, Air Products) was passed through a trap containing a molecular sieve before entering the flow system or before use in the preparation of mixtures. The molecular sieve was periodically heated to about 220 °C under vacuum. F_2 (99.9%, Cryogenic Rare Gases, 5% in He) and CH_4 (99.9995%, MG Industries) were used as provided without further purification. Cl_2 (VLSI 4.8 grade, Air Products) and C_2H_6 (99.95%, MG Industries) were degassed at liquid nitrogen temperature.

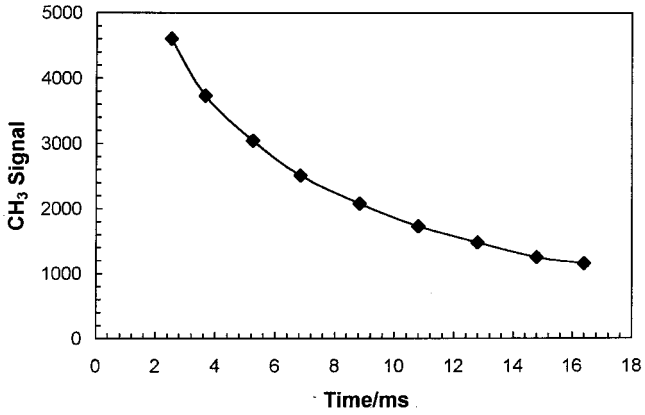

Figure 1. Plot of CH_3 signal vs reaction time at $T = 202$ K and $P =$ 1.0 Torr He. $[CH_3]_0 = 4.35 \times 10^{12}$ molecule cm^{-3}.

Results

Figure 1 shows a typical experimental temporal profile of CH_3 signal at $T = 202$ K and $P = 1$ Torr He measured at $m/z = 15$. The reaction time (t) was derived from the measured distance (x) between the tip of the movable injector to the sampling pinhole, and the linear velocity (v) calculated from the measured pressures and gas flows:

$$\text{time } (t) = \frac{\text{distance } (x)}{\text{velocity } (v)} \tag{5}$$

Each experiment consisted of two parts: (1) the high [CH_3] ($\{1-10\} \times 10^{12}$ molecule cm^{-3}) decay measurement to determine the rate constant k_1 and the measurement of $[CH_3]_0$ via F-atom titration with Cl_2; (2) the low [CH_3] ($\sim 3 \times 10^{11}$ molecule cm^{-3}) decay measurement to determine the scaling factor (SF) along with its F-atom titration. In the majority of the experiments, the low methyl decay measurement to determine SF was performed both before and after the high methyl decay experiment. For the SF determination, the ln(CH_3 signal) versus time was fitted by the linear regression analysis in the Excel spreadsheet program to determine the intercept. The SF is the $[CH_3]_0$ from the titration divided by the intercept. For the rate constant decay curve at high [CH_3], the inverse of the CH_3 signal versus time was similarly fitted in Excel according to the second-order rate equation

$$\frac{1}{[CH_3]} = 2k_1t + \frac{1}{[CH_3]_0} \tag{6a}$$

Since [CH_3] is the product of the CH_3 signal and the scaling factor SF, this can be written as

$$\frac{1}{CH_3 \text{ signal}} = 2k_1\text{SF}t + \frac{1}{CH_3 \text{ signal } (t=0)} \tag{6b}$$

The second-order plots using eq 6b were essentially linear at both $T = 298$ and 202 K; Figure 2 shows a second-order plot of the data displayed in Figure 1 for an experiment at $T = 202$ K and $P = 1$ Torr He. The slopes of these second-order plots provided a value for k_1, but the small intercepts were poor estimates of the CH_3 signal at $t = 0$. Since this treatment neglects first-order removal of CH_3 via wall loss and reaction with residual F_2 (see below), such graphs provided an indication that these first-order processes are small and the experiment had predominately second-order behavior.

As a check on the simple graphical method, the rate constant k_1 for the methyl self-recombination was derived by a one-

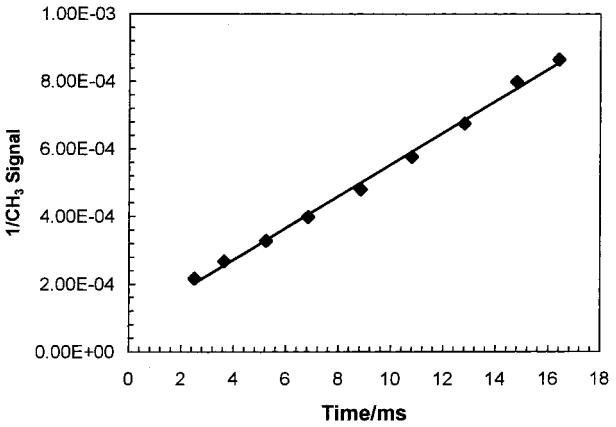

Figure 2. Plot of the reciprocal of the CH_3 signal vs reaction time at $T = 202$ K and $P = 1.0$ Torr He. Data from Figure 1.

parameter fitting of the rate constant decay curve to a numerical simulation of the reaction system using the Facsimile program.[22] The absolute concentrations of CH_3 were calculated from the net CH_3 mass spectrometric signals multiplied by the scaling factor (SF). The reaction mechanism used in the numerical simulation was the following:

$$F + CH_4 \rightarrow CH_3 + HF \text{ (ref 19)} \quad (2)$$

$$CH_3 + CH_3 + M \rightarrow C_2H_6 + M \quad (1)$$

$$CH_3 + \text{wall} \rightarrow \text{products} \quad (7)$$

$$CH_3 + F_2 \rightarrow CH_3F + F \text{ (ref 23)} \quad (8)$$

According to the numerical simulation, reaction 1 accounted for >90% of the loss of CH_3 while reactions 7 and 8 contributed <10% and <1%, respectively. This confirms the expectation from the simple graphical analysis using eq 6b. The rate constant for the first-order wall loss is very small and a temperature independent value $k_7 = 10\ s^{-1}$ was estimated from prior work[24] as well as a two-parameter fit (k_1 and k_7) to a typical experiment. The final value for k_1 is very insensitive to the value chosen for k_7.

At $T = 298$ K the graphical method using eq 6b and the numerical simulation using reactions 2, 1, 7, and 8 gave average k_1 values that agreed to within a few percent. However, at $T = 202$ K, the numerical simulation always led to values of k_1 that were on average 25% lower than the graphical method. A very likely explanation is that, at the lower temperature, diffusional mixing of CH_4 into the F/He flow is slower and formation of CH_3 via reaction 2 is considerably longer than the 0.1 ms calculated from k_2 and $[CH_4]$. Based on a rough estimate, the time scale for mixing was estimated to be at least 1 ms. When this was incorporated into the Facsimile numerical simulation, the residual sum of squares for the fit decreased substantially and the distribution of the residuals with reaction time was much flatter. Equally significant was the fact that, for a typical experiment, the fitted value for k_1 was now in much better agreement (better than 10%) with the graphical determination. We also showed that, for the plot of typical data using eq 6b, a shift in $t = 0$ by +1 ms had no effect on the slope and hence on the value of k_1. Because of this mixing complication, we prefer the simple graphical method using eq 6b to determine k_1 at both temperatures.

A factor that would adversely affect the CH_3 decay experiments is formation of stabilized but not equilibrated C_2H_6 in reaction 1 and subsequent dissociative ionization to CH_3^+ in the ionization region. The relative cracking patterns were measured at an ionization energy of 15 eV for ethane formed in situ from reaction 1 and then for a comparable concentration of ethane introduced from a 1% C_2H_6 in He mixture. Relative ratios were determined for m/z of 30, 29, 28, and 26 and were the same whether ethane arose from reaction 1 or from the prepared gas mixture. We thus have no evidence for any contribution from stabilized, nonequilibrated ethane.

TABLE 1: Summary of Experimental Conditions and Rate Data for the $CH_3 + CH_3$ Reaction at $T = 298$ K and $P = 0.6$ and 1.0 Torr He

pressure/Torr	$[CH_3]_0/10^{12}$ molecule cm^{-3}	$[CH_4]_0/[F]_0$	$k_1/10^{-11}$ cm^3 molecule $^{-1}$ s^{-1}
0.6	6.33	138	1.95
	7.60	119	2.35[a]
			<2.15 ± 0.42>[b]
1.0	5.89	90	2.34
	6.07	105	2.64
	6.77	123	2.60
	7.18	110	2.23
	7.35	97	2.35
	7.58	91	2.93
	7.66	98	2.38
	7.66	115	1.82
	7.97	84	2.66
	9.24	89	2.43
	9.49	95	2.85
	9.74	92	2.45
			<2.44 ± 0.52>[b]

[a] Value of k_1 at $P = 0.6$ Torr measured relative to average value of k_1 at $P = 1.0$ Torr for this experiment only; all other experiments are absolute measurements of k_1. [b] Mean central value of k_1 at each pressure; error is one standard deviation ($\pm 1\sigma$) plus an additional 10% for systematic errors.

$CH_3 + CH_3$ Rate Constant at $T = 298$ K. Although there are numerous measurements of k_1 at room temperature, there are only a few published studies at $P = 1$ Torr with He as the bath gas.[16] We measured k_1 at $T = 298$ K partly to fill in this gap and partly to test our experimental technique before performing measurements at lower temperatures. The ratio of $[CH_4]$ to [F] was ≅100 to ensure rapid formation of CH_3 via reaction 2 and to eliminate secondary chemistry such as the reaction of F with CH_3. The rate constant was invariant with $[CH_3]$ between $(5.9-9.7) \times 10^{12}$ molecule cm^{-3}, but was not invariant above this concentration limit. Table 1 presents the results for $T = 298$ K and $P = 0.6$ and 1.0 Torr He. The rate constant k_1 was determined to be $(2.15 \pm 0.20) \times 10^{-11}$ cm^3 $molecule^{-1}$ s^{-1} at $P = 0.6$ Torr He and $(2.44 \pm 0.28) \times 10^{-11}$ cm^3 $molecule^{-1}$ s^{-1} at $P = 1.0$ Torr He where the quoted errors are one standard deviation ($\pm 1\sigma$). To allow for systematic errors we add an additional 10%. Therefore, the recommended values are k_1 (0.6 Torr) $= (2.15 \pm 0.42) \times 10^{-11}$ cm^3 $molecule^{-1}$ s^{-1} and k_1 (1.0 Torr) $= (2.44 \pm 0.52) \times 10^{-11}$ cm^3 $molecule^{-1}$ s^{-1}. The results suggest a slight positive dependence of k_1 on pressure over this narrow range, consistent with most previous studies with M = He or Ar.

$CH_3 + CH_3$ Rate Constant at $T = 202$ K. At $T = 202$ K, the rate constant for methyl recombination k_1 was measured at pressures of 0.6, 1.0, and 2.0 Torr as shown in Table 2. At this temperature, $[CH_4]/[F] = 100-600$. For $P = 1$ Torr, k_1 is invariant for initial methyl concentrations in the range $(1.2-8.6) \times 10^{12}$ molecule cm^{-3}. The average value is $k_1 = (5.25 \pm 1.43) \times 10^{-11}$ cm^3 $molecule^{-1}$ s^{-1} where the error is 1σ (statistical) + 15% (systematic). This result is ~2 times higher than that at 298 K. Because of the temperature gradient in the region near the sampling pinhole ($d = 1-10$ cm) described in

TABLE 2: Summary of Experimental Conditions and Rate Data for the $CH_3 + CH_3$ Reaction at $T = 202$ K and $P = 0.6$, 1.0 and 2.0 Torr He

pressure/Torr	$[CH_3]_0/10^{12}$ molecule cm^{-3}	$[CH_4]_0/[F]_0$	$k_1/10^{-11}$ cm^3 molecule $^{-1}$ s^{-1}
0.6	5.73	142	4.62
	7.23	119	5.38
	8.56	98	5.12
			$< 5.04 \pm 1.15 >^a$
1.0	1.21	589	5.98
	1.86	384	5.44
	2.69	272	5.53
	3.57	199	5.26
	4.35	105	5.00
	5.84	97	5.37
	6.42	107	4.25
	6.99	129	5.74
	7.60	117	4.52
	8.21	99	6.24
	8.62	100	4.45
			$< 5.25 \pm 1.43>^a$
2.0	3.11	234	6.68
	6.26	115	5.89
	10.3	97	6.98
			$< 6.52 \pm 1.54 >^a$

[a] Mean central value of k_1 at each pressure; error is one standard deviation ($\pm 1\sigma$) plus an additional 15% for systematic errors.

the Experimental Section and because of the complications from the corrections applied, we made two additional measurements of k_1 at $T = 202$ K, $P = 1.0$ Torr He using a recently installed flow tube in which the jacketed region went all the way to the end of the flow tube. The design of the new flow reactor, to be described in a future publication, resulted in a uniform temperature profile. Thus there was complete absence of the previously discussed corrections due to the temperature gradient. The values of k_1 at $P = 1.0$ Torr were 5.51 and 5.21 in units 10^{-11} cm^3 $molecule^{-1}$ s^{-1}. These are within 5% of the central value of 5.25×10^{-11} cm^3 $molecule^{-1}$ s^{-1} for the 11 experiments (Table 2) obtained after correction for the effect of the temperature gradient. This demonstrates the essential validity of the corrections applied.

The measured value at $P = 0.6$ Torr is $k_1 = (5.04 \pm 1.15) \times 10^{-11}$ cm^3 $molecule^{-1}$ s^{-1} and at $P = 2.0$ Torr, $k_1 = (6.52 \pm 1.54) \times 10^{-11}$ cm^3 $molecule^{-1}$ s^{-1} with the same error estimate of $1\sigma + 15\%$. The systematic error was increased somewhat compared to that at $T = 298$ K to allow for the additional difficulties of the measurements at $T = 202$ K. Over this small pressure range the results suggest a slight increase with increasing pressure which indicates that, as expected, the reaction is in the falloff region.

Discussion

The only published experimental measurements with which our results at $T = 298$ K and $P = 1$ Torr He may be directly compared are those of Deters et al.[16a,b] and Stoliarov et al.[16c] These studies were designed to measure the rate constant for the radical−radical reactions $CH_3 + OH$,[16a] $CH_3 + CH_2$,[16b] and $CH_3 + C_2H_3$[16c] with $[CH_3] > [OH, CH_2$ or $C_2H_3]$, and thus these determinations of k_1 for $CH_3 + CH_3$ were a byproduct of the measurements. Nevertheless, their results of $k_1 = (2.9 \pm 0.8)$,[16a] (2.9 ± 0.8),[16b] and (3.5 ± 0.5)[16c] $\times 10^{-11}$ cm^3 $molecule^{-1}$ s^{-1} are in reasonable agreement with our value $k_1 = (2.4 \pm 0.5) \times 10^{-11}$ cm^3 $molecule^{-1}$ s^{-1} given the quoted uncertainties. All other published studies at room temperature are at higher pressures of He[4] or with the bath gas M = Ar.[3−5] We recently learned of an unpublished DF−MS study[25] at $T = 298$ K and $P = 1$ Torr He which yields $k_1 = 2.6 \times 10^{-11}$ cm^3 $molecule^{-1}$ s^{-1}, in excellent agreement with our determination. At $T = 298$ K and $P = 0.55$ Torr He, the Deters et al.[16a] result of $k_1 = (1.8 \pm 0.7) \times 10^{-11}$ cm^3 $molecule^{-1}$ s^{-1} is in good agreement with our value $k_1 = (2.2 \pm 0.4) \times 10^{-11}$ cm^3 $molecule^{-1}$ s^{-1} at $P = 0.6$ Torr He.

TABLE 3: Lennard-Jones Parameters and Calculated Collision Numbers

collision partners $(\sigma, \epsilon)^a$	$k_{12}(T)$ /cm^3 $molecule^{-1}$ s^{-1}, $\Omega^{(2,2)*}$	
	$T = 200$ K	$T = 296$ K
Ar(3.42, 124) + C_2H_6(4.42, 230)	3.47×10^{-10} [b], 1.45	3.58×10^{-10} [b], 1.23
He(2.58, 10.2) + C_2H_6(4.42, 230)	4.06×10^{-10}, 0.97	4.55×10^{-10}, 0.89

[a] Units of Angstroms and Kelvin, respectively. [b] Present calculated values in agreement with those used by ref 10.

Of more interest is the data at $T = 202$ K that provides the first measure of the pressure dependence of k_1 for a temperature below $T = 298$ K. Qualitatively, our results demonstrate that the reaction is in the falloff region. Moreover, the measured value of the rate constant at $P = 2.0$ Torr He, $k_1 = (6.5 \pm 1.5) \times 10^{-11}$ cm^3 $molecule^{-1}$ s^{-1}, is very close to the previously measured value[5] of the high-pressure limit at $T = 200$ K, $k_\infty = (6.9 \pm 0.2) \times 10^{-11}$ cm^3 $molecule^{-1}$ s^{-1}. This suggests that at $P = 2.0$ Torr He the measured k_1 is very close to or has reached k_∞. Other than this reference to the value for k_∞, comparison with previous data at $T = 202$ K is not an option. So we turn to a comparison with calculations of the rate constant under the conditions of our experiment.

Calculations for the "observed" rate coefficients for the combination of methyl radicals in an argon bath ($T = 200-1600$ K) have been reported by Klippenstein and Harding[10] (KH) as a function of the energy removed per collision. In the following discussion the numerical value associated with the average energy removed per collision is defined as a positive quantity, i.e., $-\langle\Delta E\rangle_d$. As shown below, the argon pressures can be transformed to the equivalent helium pressures using the appropriate Lennard-Jones parameters (σ, $\Omega^{(2,2)*}$ and ϵ)[26] for the collision partners. Bimolecular collision rate coefficients (cm^3 $molecule^{-1}$ s^{-1}) are determined by temperature, collision cross section (σ), well depth (ϵ), masses (m_1 and m_2), and the collision integral ($\Omega^{(l,s)*}$). For vibrational energy transfer it has been *assumed* that l,s = 2,2. Thus the collision frequencies, $k_{12}(T)$, between substrate (1) and deactivator (2) are calculated from the expression

$$k_{12}(T) = \pi[\sigma_1/2 + \sigma_2/2\,]^2\,[8kT(m_1 + m_2)/(\pi m_1 m_2)]^{0.5}\,\Omega^{(2,2)*}\,[T/(\epsilon_1\,\epsilon_2)^{0.5}] \quad (9)$$

A tabulation of $k_{1,2}(T)$ and the appropriate constants for the Lennard-Jones 6−12 potential are presented in Table 3. The equivalent helium pressure is calculated by

$$p(\mathrm{He}) = cp(\mathrm{Ar}) \quad (10)$$

where $c = [(\sigma_1 + \sigma_{Ar})^2/(\sigma_1 + \sigma_{He})^2]\,[(m_1 + m_{Ar})/(m_1 + m_{He})]^{0.5}\,[m_{He}/m_{Ar}]^{0.5}\,[\Omega(T/(\epsilon_1\,\epsilon_{Ar})^{0.5})/\Omega(T/(\epsilon_1\epsilon_{He})^{0.5})]$. The conversion factor, c, changes from 0.856 to 0.787 as the temperature increases from 200 to 296 K. To be noted is that the bracketed σ and mass factors, which are independent of temperature, give a factor of 0.562 while the bracketed Ω factor is 1.49 at 200 and decreases to 1.38 at 296 K. Thus, the assumed values for the parameters of $k_{12}(T)$ and its temperature dependence will systematically displace the k vs pressure "falloff" curves.

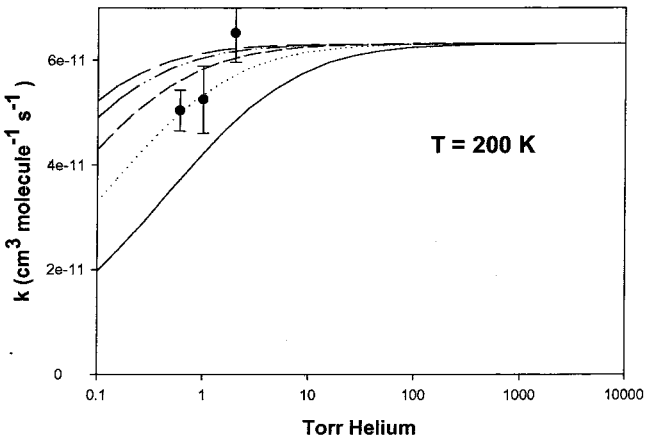

Figure 3. Plots of calculated k_1 vs pressure of He at T= 200 K for values of $-\langle\Delta E\rangle_d$ (cm^{-1}): long dashed line (800), dash−dot-dot line (400), short dashed line (200), dot-dot line (100), solid line (50). Experimental results (filled circles) at P = 0.6, 1.0, and 2.0 Torr He and T = 202 K are from this study (Table 2).

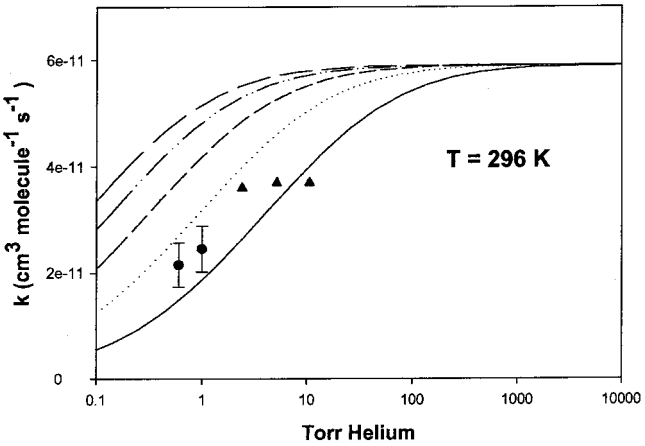

Figure 4. Plots of calculated k_1 vs pressure of He at T = 296 K for values of $-\langle\Delta E\rangle_d$ (cm^{-1}): long dashed line (800), dash−dot-dot line (400), short dashed line (200), dot-dot line (100), solid line (50). Experimental results (filled circles) at P = 0.6 and 1.0 Torr He and T = 298 K are from this study (Table 1). Experimental results (filled triangles) at P = 2.5, 5.2 and 10.7 Torr He and T = 296 K are from ref 4.

The falloff curves in Figures 3 and 4 are the results of transforming the KH curves[10] as a function of $-\langle\Delta E\rangle_d$ from argon to helium at T = 200 and 296 K, respectively. The new plots exhibit the same information as those with argon as the deactivator; the falloff extends to higher pressure as $-\langle\Delta E\rangle_d$ decreases and/or the temperature increases. Also to be noted is that for a given $-\langle\Delta E\rangle_d$ the falloff curves are shifted to lower pressure when the deactivator changes from argon to helium, since $c < 1$.

Since the exact value for $-\langle\Delta E\rangle_d$ for this reaction and its temperature dependence are not known, other systems must be used to get some insight. The decomposition of ethyl radicals formed by the addition of H atoms to ethene is a system comparable to the methyl radical combination. The similarity is that both systems have nearly the same number of atoms and the excess energy (average thermal energy of the chemically activated species minus the critical energy for the reverse of the formation) is very small, comparable to the available thermal energy. The differences are the level of excitation (∼40 kcal mol^{-1} for the ethyl radicals and ∼85 kcal mol^{-1} for the ethane) and the unpaired electron. Data from other systems suggest that the unpaired electron does not affect the vibrational energy transfer model and the excess energy is more important than the excitation energy.[27] In the ethyl radical system[28] the collision efficiency, β_c, decreases from 0.37 to 0.26 as the temperature increases from 195 to 300 K; $-\langle\Delta E\rangle_d$ values were not reported for this system. The deactivation of butyl radicals[29] formed by the addition of H atoms to *cis*-2-butene has been studied with both helium and argon as the deactivators at T = 195 and 300 K; this system has ∼40 kcal mol^{-1} of internal energy and an excess energy of ∼7 kcal mol^{-1}. The results from those experiments indicate that β_c for helium decreases from 0.55 to 0.35 as the temperature increase from 195 to 300 K; similarly, β_c for argon decreases from 0.59 to 0.41 over the same temperature range. The values for $-\langle\Delta E\rangle_d$ for helium decreased from 2.1 to 1.5 kcal mol^{-1} as the temperature increased from 195 to 300 K. Over the same temperature range $-\langle\Delta E\rangle_d$ for argon increased from 2.1 to 2.6 kcal mol^{-1}. The decrease in β_c with increase in temperature is due to the increase of the "up" transitions with increasing temperature. These results suggest a weak or negligible (within experiment error) temperature dependence for $-\langle\Delta E\rangle_d$ and a small difference between argon and helium deactivators. The energy transfer information reported in the combination of substituted methyl radicals[30] was not considered pertinent. Although they have comparable average excitation energies these systems have average excess energies in excess of 20 kcal mol^{-1} (substantially greater than the available thermal energy). These large excess energies require a multicollision cascade for stabilization, which produces large nonlinearities on the yield of stabilization with pressure.[27]

The KH plots at T = 200 K indicate that the reported experiments[5] with argon as the deactivator are in the high-pressure limit so that energy transfer parameters cannot be extracted. However, at T = 296 K the lowest pressure experimental rate coefficient for argon has decreased by more than a factor of 3 from its high-pressure limit; the measured falloff for argon is consistent with $-\langle\Delta E\rangle_d$ between 100 and 200 cm^{-1}. Values for $-\langle\Delta E\rangle_d$ can also be extracted from the present experiments with helium by assuming the same high-pressure rate coefficients as calculated by KH. At T = 200 K the lowest pressure rate coefficient (∼0.8 times the rate coefficient for the high-pressure limit) is consistent with $-\langle\Delta E\rangle_d$ ∼100 cm^{-1} as shown in Figure 3. Similar reasoning for the T = 296 K helium experiments indicates a value of $-\langle\Delta E\rangle_d$ between 50 and 100 cm^{-1} as shown in Figure 4. Thus the present helium experiments suggest a slight increase in $-\langle\Delta E\rangle_d$ with decreasing temperature, with $-\langle\Delta E\rangle_d$ being approximately half of that for argon. These values of $-\langle\Delta E\rangle_d$ for helium are also 2 to 4 times smaller than those observed for the H + *cis*-2-butene system.[29] However, it is difficult to uniquely identify the experimental points displaced from the calculated curves as due to either a change in $-\langle\Delta E\rangle_d$ or to the temperature dependence of $\Omega^{(2,2)*}$. Likewise, an error in σ_2 would also produce a displacement in the pressure curves.

Finally, a brief consideration may be given to the implication of these results for the modeling of the hydrocarbon chemistry in the atmospheres of the planets Saturn and Neptune. As mentioned in the Introduction, attempts to compare the observed concentration of the methyl radical in the atmospheres of these planets[11,12] with those predicted by atmospheric models have led to the suggestion[11−14] that the loss of CH_3 via the reaction $CH_3 + CH_3$ (1) was significantly underestimated due to inappropriate values for k_1 based on the limited laboratory data available for this reaction at low temperatures and low pressures. The danger of extrapolating laboratory data to temperatures and pressures far beyond the range of the experiments is widely

recognized. The present experiments at $T = 202$ K over a limited range of low pressures seems to affirm the validity of the Klippenstein and Harding calculations[10] in the falloff region as extended here for M = He. This suggests that, in models of the hydrocarbon chemistry of the outer planet atmospheres, use of this theoretical calculation for k_1 is preferable to extrapolating the limited laboratory data available.

Acknowledgment. This work was supported by the NASA Planetary Atmospheres Research Program. R.P.T., Jr. thanks the National Academy of Sciences for the award of a postdoctoral research associateship. We thank Stephen Klippenstein and Larry Harding for their generosity in sharing with us their calculated falloff curves for argon. We thank Jozef Peeters for informing us of the unpublished measurement of k_1(298 K) at $P = 1.0$ Torr He. We thank Paul Romani for bringing this problem to our attention and for helpful discussions. Informative discussions with Sushil Atreya, Yuk Yung, and Julie Moses are also gratefully acknowledged.

References and Notes

(1) Mallard, W. G. NIST Chemistry Web Book, NIST Stand. Ref. Database No. 69-1998 (http://webbook.nist.gov/chemistry).

(2) Gomer, R.; Kistiakowsky, G. B. *J. Chem. Phys.* **1951**, *19*, 85.

(3) Macpherson, M. T.; Pilling, M. J.; Smith, M. J. C. *Chem. Phys. Lett.* **1983**, *94*, 430. Macpherson, M. T.; Pilling, M. J.; Smith, M. J. C. *J. Phys. Chem.* **1985**, *89*, 2268.

(4) Slagle, I. R.; Gutman, D.; Davies, J. W.; Pilling, M. J. *J. Phys. Chem.* **1988**, *92*, 2455.

(5) Walter, D.; Grotheer, H.-H.; Davies, J. W.; Pilling, M. J.; Wagner, A. F. *Twenty-Third Symposium (International) on Combustion*; The Combustion Institute: Pittsburgh, PA, 1990; p 107.

(6) Wardlaw, D. M.; Marcus, R. A. *J. Phys. Chem.* **1986**, *90*, 5383; erratum, *J. Phys. Chem.* **1987**, *91*, 4864.

(7) Wagner, A. F.; Wardlaw, D. M. *J. Phys. Chem.* **1988**, *92*, 2462.

(8) Forst, W. *J. Phys. Chem.* **1991**, *95*, 3612.

(9) Robertson, S. H.; Pilling, M. J.; Baulch, D. L.; Green, N. J. B. *J. Phys. Chem.* **1995**, *99*, 13452.

(10) Klippenstein, S. J.; Harding, L. B. *J. Phys. Chem. A* **1999**, *103*, 9388.

(11) Bezard, B.; Feuchtgruber, H.; Moses, J. I.; Encrenaz, T. *Astron. Astrophys.* **1998**, *334*, L41.

(12) Bezard, B.; Romani, P. N.; Feuchtgruber, H.; Encrenaz, T. *Astrophys. J.* **1999**, 515, 868.

(13) Atreya, S. K.; Edington, S. G.; Encrenaz, T.; Feuchtgruber, H. *The Universe as Seen by ISO, Eur. Space Agency Spec. Publ.*, ESA SP-427, 1999; p 149.

(14) Lee, A. Y. T.; Yung, Y. L.; Moses, J. *J. Geophys. Res.* **2000**, *105*, 20207.

(15) Parkes, D. A.; Paul, D. M.; Quinn, C. P. *J. Chem. Soc., Faraday Trans. I* **1976**, *72*, 1935.

(16) (a) Deters, R.; Otting, M.; Wagner, H. Gg.; Temps, F.; Laszlo, B.; Dobe, S.; Berces, T. *Ber. Bunsen-Ges. Phys. Chem.* **1998**, *102*, 58. (b) Deters, R.; Otting, M.; Wagner, H. Gg.; Temps, F.; Dobe, S. *Ber. Bunsen-Ges. Phys. Chem.* **1998**, *102*, 978. (c) Stoliarov, S. I.; Knyazev, V. D.; Slagle, I. R. *J. Phys. Chem. A* **2000**, *104*, 9687.

(17) Brunning, J.; Stief, L. J. *J. Chem. Phys.* **1986**, *84*, 4371.

(18) Nesbitt, F.; Payne, W. A.; Stief, L. J. *J. Phys. Chem.* **1988**, *92*, 4030.

(19) DeMore, W. B.; Sander, S. P.; Golden, D. M.; Hampson, R. F.; Kurylo, M. J.; Howard, C. J.; Ravishankara, A. R.; Kolb, C. E.; Molina, M. J. *Chemical Kinetics and Photochemical Data for Use in Stratospheric Modeling:* Evaluation Number 12, NASA Panel for Data Evaluation, JPL Publication 97-4, 1997.

(20) Unpublished results from CNRS, Orleans and GSFC, Greenbelt to be submitted to *J. Phys.Chem.*

(21) Leone, S. R.; Kovalenko, L. J. *J. Chem. Phys.* **1984**, *80*, 3656. Timonen, R. S.; Gutman, D. *J. Phys. Chem.* **1986**, *90*, 2987.

(22) Curtis A. R.; Sweetenhan, W. P. Facsimile program. Report R-12805; U. K Atomic Energy Research Establishment, Harwell, 1987.

(23) Moore, C. M.; Smith, I. W. M.; Stewart, D. W. A. *Int. J. Chem. Kinet.* **1994**, *26*, 813.

(24) Thorn, R. P.; Payne, W. A.; Stief, L. J.; Tardy, D. C. *J. Phys. Chem.* **1996**, *100*, 13594. Seakins, P. W.; Robertson, S. H.; Pilling, M. J.; Wardlaw, D. M.; Nesbitt, F. L.; Thorn, R. P.; Payne, W. A.; Stief, L. J. *J. Phys. Chem. A* **1997,** *101*, 9974.

(25) Peeters, J., private communication, July 2000.

(26) Hirschfelder, J. O.; Curtiss, C. F.; Bird, R. B. *Molecular Theory of Gases and Liquids*; John Wiley & Sons: New York, 1967.

(27) Tardy, D. C.; Rabinovitch, B. S. *Chem. Rev.* **1977**, *77*, 369.

(28) Current, J. H.; Rabinovitch, B. S., *J. Chem. Phys.* **1964**, *40*, 2742.

(29) Kohlmaier, G.; Rabinovitch, B. S. *J. Chem. Phys.* **1963**, *38*, 1692, 1709.

(30) Oref, I.; Tardy, D. C. *Chem. Rev.* **1990**, *90*, 1407.